MEASUREMENT OF THE IMPEDANCE OF FROG SKELETAL MUSCLE FIBERS

R. VALDIOSERA, C. CLAUSEN, and R. S. EISENBERG

From the Department of Physiology, University of California at Los Angeles, Los Angeles, California 90024

ABSTRACT Impedance measurements are necessary to determine the passive electrical properties of cells including the equivalent circuits of the several pathways for current flow. Such measurements are usually made with microelectrodes of high impedance (some 15 MΩ) over a wide frequency range (1–10,000 Hz) and so are subject to many errors. An input amplifier has been developed which has negligible phase shift in this frequency range because it uses negative feedback to keep tiny the voltage on top of the microelectrode. An important source of artifact is the extracellular potential produced by capacitive current flow through the wall of the microelectrodes and the effective resistance of the bathing solution. This artifact is reduced some 10 times by shielding the current microelectrode with a conductive paint. The residual artifact is analyzed, measured, and subtracted from our results. The interelectrode coupling capacitance is reduced below 2×10^{-17} F and can be neglected. Phase and amplitude measurements are made with phase-sensitive detectors insensitive to noise. The entire apparatus is calibrated at different signal to noise ratios and the nature of the extracellular potential is investigated. The phase shift in the last 5–20 μm of the microelectrode tip is shown to be small and quite independent of frequency under several conditions. Experimental measurements of the phase characteristic of muscle fibers in normal Ringer are presented. The improvements in apparatus and the physiological significance of impedance measurements are discussed. It is suggested that the interpretation of impedance measurements is sensitive to small errors and so it is necessary to present objective evidence of the reliability of one's apparatus and measurements.

INTRODUCTION

The passive electrical properties of frog skeletal muscle have been studied in some detail (Katz, 1948; Fatt and Katz, 1951; Falk and Fatt, 1964; Freygang et al., 1967; Gage and Eisenberg, 1969; Schneider, 1970; Hodgkin and Nakajima, 1972 *a*, 1972 *b*; Mobley et al., 1973; Peachey and Adrian, 1973) since they are intimately related to the mechanism by which an action potential on the surface membrane initiates contraction in the depths of a muscle fiber. The transverse tubular system, or T-system for short, is the channel by which current flows into the depths of the fiber and so the electrical properties of this system have received particular attention.

There is still much uncertainty, however, concerning the electrical properties of the tubular system: for instance, we do not know how much current enters the T-system nor do we know in detail how that current spreads down the tubules.

In order to answer these questions one needs precise experimental data concerning the passive electrical properties of muscle fibers. In some experiments designed to measure these properties current has been applied outside the muscle fiber and measurements have been made of the change in the flow of this extracellular current produced by the fiber (Bozler and Cole, 1935; Fatt, 1964; Freygang and Gunn, 1973). Such experiments often prove to be difficult to interpret since the pattern of current flow around a muscle fiber is not known and the prediction of such flow seems to be a formidable theoretical problem even for oversimplified models of the fiber. Experiments have also been performed by applying current to the inside of the muscle fiber with a glass micropipette filled with highly conductive salt solution. The applied current flows along the axis of the fiber and then across the membrane to be collected in an "indifferent" bath electrode. The potential produced within the fiber by this flow of current is measured with another microelectrode and the relation between current applied and potential recorded can be used to describe the electrical properties of the fiber. This method has the considerable advantage that the pattern of current flow can be analyzed with a reasonably simple theory (one-dimensional cable theory: Jack et al., 1973; Peachey and Adrian, 1973); more realistic models of current flow can also be analyzed without overwhelming difficulties (Eisenberg and Johnson, 1970; Peskoff et al., 1972). The main difficulty with the method concerns the properties of the glass micropipettes: they must be tiny and so have a high impedance to current flow, of the order of tens of megohms, and tend to be nonlinear. Since it is necessary to measure the electrical properties over a wide range of time or frequency, the flow of current in the unavoidable stray capacitances surrounding these microelectrodes becomes important. Indeed, the limiting factor in the determination of the pattern of current flow in a muscle fiber is the uncertainty associated with these stray capacitances. We therefore devote much of this paper to a description of a particular experimental apparatus which removes most of these problems and to an analysis of the remaining difficulties and residual errors.

Having decided that measurements should be made of the potential within the muscle fiber produced by current applied within the fiber, one must choose a particular waveform of current. Two waveforms have commonly been used in physiological experiments, sinusoids and step functions, although other waveforms, particularly random noise, have significant advantages, at least in principle (Bendat and Piersol 1971). The advantage of step functions is that the experiments can be performed quite quickly and conveniently with readily available equipment; the disadvantage is that it is difficult to distinguish between different electrical models because of the nature of the exponential functions which describe the response of a linear lumped network to step function input (Lanczos, 1957). (A lumped network

is one which contains a finite number of circuit elements.) Another important disadvantage is the difficulty involved in making theoretical predictions concerning the transient response of complicated networks. Sinusoidal waveforms do not present these problems since they allow both the accurate identification and relatively simple analysis of complicated circuits. Sinusoidal waveforms have these advantages essentially because it is not necessary to describe explicitly the time dependence of the wave-forms: if a sinusoidal current or voltage is applied to a linear time invariant system, every current and voltage in the system is a sinusoid of the same frequency (Zadeh and Desoer, 1963, p. 418). The main disadvantage of sinusoidal currents is that measurements must be made at one frequency at a time. Measurements covering a reasonable bandwidth with reasonable resolution take considerable time and require the preparation to be very stable. Another disadvantage is that sinusoidal waveforms require special equipment and special analysis; it is our opinion, however, that this disadvantage is more illusory than real since experiments *of equivalent precision* using step functions are likely to require at least as much specialized equipment and analysis.

A sinusoid of known frequency is specified by its amplitude and phase, and indeed in the first impedance measurements with microelectrodes both parameters were measured (Falk and Fatt, 1964; Eisenberg, 1967). If one wishes to identify the equivalent circuit of a lumped linear passive network with just two terminals, it is not necessary, however, to measure both the amplitude and the phase of the signal because the amplitude at any frequency can be calculated (within one scale factor independent of frequency) from an integral relation involving the phase angle measured at all frequencies (Tuttle [1958] gives these relations in a particularly clear manner: eq. 8.07–9 and Tables 8.08-A and 8.08-B). The qualitative meaning of the integral relations is that the phase angle at frequency f is given by the slope (at frequencies near f) of the curve relating amplitude and frequency. Thus, the plot of phase vs. frequency is in a certain sense the derivative of the plot of amplitude vs. frequency. The phase plot then usually shows more fine structure than the amplitude plot and is a more precise tool for specifying most electrical networks.

It is usually more convenient to determine the amplitude by another method which does not require the explicit evaluation of an integral (van Valkenburg, 1960, Sec. 8.5). In this method one chooses an impedance function which fits the phase data (in the biological case one usually chooses an impedance function which describes an anatomically reasonable equivalent circuit as well as fits the data). It is then always possible, for two terminal lumped networks, to determine from the phase data alone all the parameters of the circuit except one. The undetermined parameter is a scaling factor, independent of frequency, which can be determined from one amplitude measurement at any convenient frequency; usually, the scale factor is determined from amplitude data at zero or infinite frequency.

In this manner the impedance function which describes a two terminal lumped network can be entirely specified by phase measurements and just one amplitude measurement. The impedance function specifies the linear behavior of the circuit for

any input, e.g. for inputs of step or ramp functions of current or voltage. It can be seen then that phase measurements include all the information about a linear two-terminal circuit which might be determined from transient measurements.

The properties of the network functions just described do *not* immediately apply to the physiological case since networks of physiological interest are typically distributed; that is, they cannot be described by a finite number of circuit elements. In the particular case of interest here, in which measurements are made with the current and voltage microelectrode quite close together in a cylindrical cell with an interior assumed to be purely resistive, the entire impedance function can *in principle* be determined from phase data and one amplitude measurement by the method of van Valkenburg described above (see Freygang et al., 1967, and Valdiosera et al., 1974 *a*). The corrections for capacitive artifact require, however, measurement of both amplitude and phase and so we make both such measurements in the frequency range in which the artifact is significant.

This paper specifies and analyzes the apparatus necessary to measure the phase and amplitude of the potential recorded with a microelectrode when current is applied to a muscle fiber with another microelectrode. Another paper (Valdiosera et al., 1974 *a*) describes several electrical models of the muscle fiber, including in all models the important effect of variation of potential around the circumference of the fiber as well as along its length. Plots are given of the expected phase for a variety of values of each circuit element in each model. A method is presented for determining the value of the circuit elements of particular equivalent circuits which fit the experimental data. A third paper (Valdiosera et al., 1974 *b*) describes the experimental phase measurements from some 140 muscle fibers bathed in a variety of solutions, particularly solutions of differing conductivity. The models presented in the second paper are fitted to the data and a model is chosen which best fits the experimental data in all the solutions.

METHODS

Input Amplifier

The first experiments in which sinusoidal currents were carefully applied to a muscle fiber with a microelectrode were performed by Falk and Fatt (1964). They used an optimized version of the usual apparatus for recording potential and applying current with microelectrodes: that is, they connected the current passing microelectrode directly to an oscillator and the voltage recording microelectrode directly to a cathode follower with low input capacitance. Current was determined by measuring the potential drop produced by the flow of the current across a resistor in series with the bath. The potentials recorded by this arrangement are severely distorted by electrical artifact produced by current flow in the stray capacitances around and between the microelectrodes and large corrections must be made to the experimental data before it can be used. Unfortunately, the artifact cannot be directly measured since it depends on the unknown impedance being measured and so the equation used to correct the experimental data for the capacitive artifact has not been subject to experimental check (Eisenberg, 1967, Appendix 1). For this reason, there is considerable uncer-

tainty concerning these measurements in the frequency range (e.g. frequencies above 500 Hz) where the capacitive artifact is significant.

Freygang et al. (1967) developed another experimental arrangement which at one blow removed a number of these difficulties, at least in principle. They used an ingenious circuit, similar in principle to that shown in Fig. 1, for recording the potential within the fiber. In this circuit the voltage recording microelectrode is directly connected to the inverting input

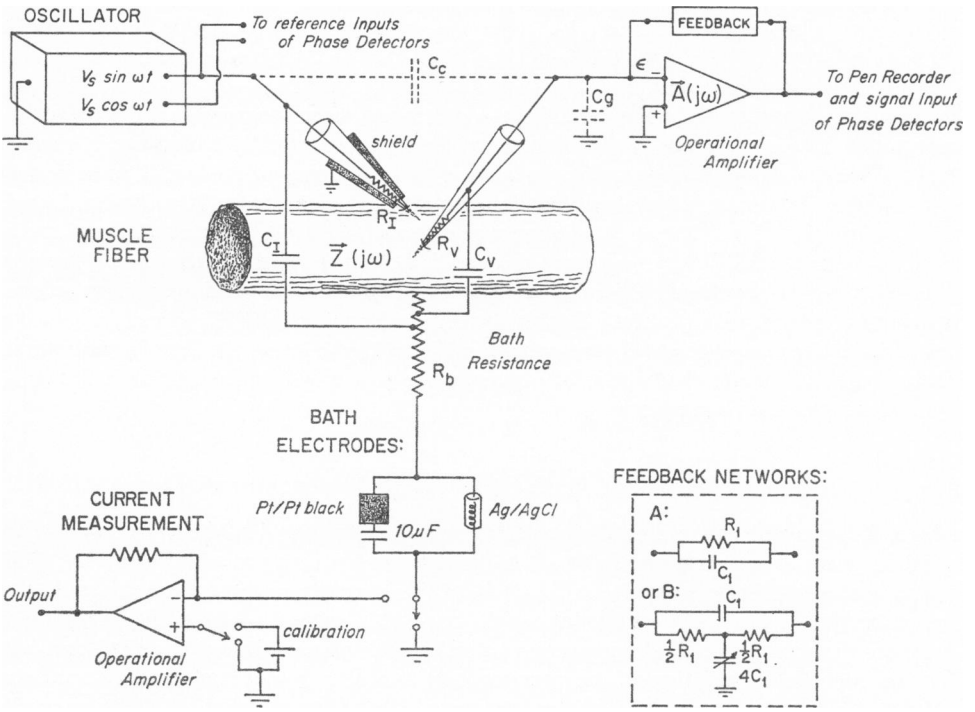

FIGURE 1 The experimental apparatus. The oscillator has two outputs, one of which serves as an input to the current microelectrode, both of which serve as reference signals to the phase sensitive detectors. The current microelectrode is shielded with a conductive paint which in turn is coated with an insulating varnish. Current flow through the walls of the microelectrodes and the resistance of the bathing solution produces significant extracellular potentials and so the effective resistance of the bathing solution is included in the circuit. The linear electrical properties of the fiber are represented by the impedance $\mathbf{Z}(j\omega)$. The arrangement of bath electrodes has negligible impedance at both high and low frequencies. The coupling capacitance is measured to be less than 2×10^{-17} F and so can be neglected. The top of the voltage recording microelectrode is held by feedback at the tiny voltage ϵ and so the current through C_g is negligible. We use feedback network B because it has minimal phase shift for a given value of C_1 (the value of which is determined by stability and noise considerations). Feedback network A has been used by Freygang et al. (1967) and Schneider (1970). The phase sensitive detectors directly measure the real and imaginary parts of the output voltage $\mathbf{V}_{obs}$ of the operational amplifier connected to the voltage microelectrode. Similar measurement of the output voltage of the current operational amplifier and of the oscillator output voltage allows measurement of R_I. Injection of a potential from the calibration battery allows measurement of R_V. The values of R_1, R_V, R_I, and $\mathbf{V}_{obs}$ determine $\mathbf{Z}_{obs}$ or ζ_{obs} and thus $\mathbf{Z}$ as described in the text.

of an operational amplifier, which input is also connected to the output of the operational amplifier through a feedback network. The current flow through the feedback network reduces the potential at the inverting node to a small but finite value (the potential at the node is shown as ε in Fig. 1) and makes negligible the current flow through the capacitance C_g. With this arrangement the correction for capacitive artifact is greatly reduced and becomes directly measurable, although there are significant problems remaining as we shall see.

In order to implement the circuit of Freygang, one must choose a feedback network which does not introduce significant artifact itself and does not contribute too much noise. The original feedback network used by Freygang et al., shown in Fig. 1 as "feedback network A," introduces a phase shift of arctan $\omega R_1 C_1$ where ω, the angular frequency of the sinusoid in radians per second, is 2π times the frequency in hertz. The DC gain of the input amplifier (output divided by the potential within the muscle fiber) is given by $-R_1/R_V$ and so in order to keep the gain near unity and thus have a reasonable signal-to-noise ratio, R_1 must be comparable to the resistance of the microelectrode, of the order of 15 MΩ. Since it is necessary to measure phase without artifact at least up to a frequency of 10^4 Hz, C_1 must be very small. In fact if the acceptable phase shift in the input amplifier is to be 1° at 10^4 Hz, then C_1 must be less than 2×10^{-14} F! It is in practice extremely difficult, but probably not impossible, to make the feedback capacitance this small, but other problems concerning the need for reasonable noise and stability in the amplifier prohibit such a small feedback capacitance in any case. The usual treatment of operational amplifiers does not allow analysis of noise and stability because it considers the operational amplifier to have infinite gain, no internal phase shift, and infinite bandwidth. We represent the gain of the operational amplifier $\mathbf{A}(j\omega)$ by the more realistic expression

$$\mathbf{A}(\mathbf{s}) = \frac{A_o}{1 + (\mathbf{s}A_o/\omega_c)} \tag{1}$$

where A_o is the gain of the amplifier at DC (a negative number when the input signal is applied only to the inverting terminal), ω_c is the angular frequency at which the gain of the operational amplifier has magnitude $[A_o/(1 + A_o)] \simeq 1$ and $\mathbf{s}$ is written as a generalization and abbreviation for $j\omega$.[1] Typical values might be $-A_o = 10^6$; $\omega_c = 4\pi \times 10^7$ rad/s. Eq. 1 describes the gain of an ideal operational amplifier with phase shift less than 90° and is in fact an imperfect description of the commercially available operational amplifiers we use. Nevertheless, analyses using this representation of $\mathbf{A}(\mathbf{s})$ illustrate most of the phenomena important in the design of operational amplifier circuits (Barna, 1971, especially Chap. 7).

The expression for the gain of the operational amplifier (Eq. 1) and Kirchoff's laws allow analysis of the response of the entire input amplifier circuit. This analysis is presented here since it has not appeared elsewhere to our knowledge and is essential to the qualitative design of operational amplifier circuits of this type.

$$\frac{\mathbf{V}_{obs}}{\mathbf{I}_V} = \frac{-\omega_c}{C_1 + C_g} \frac{1}{\mathbf{s}^2 + \mathbf{s}\dfrac{\omega_c C_1}{C_1 + C_g} + \dfrac{\omega_c}{R_1(C_1 + C_g)}}, \tag{2}$$

[1] Throughout these papers we use the standard notation of electric circuit theory (Desoer and Kuh, 1969, Chap. 7) in which potential and current are written as complex variables (indicated here with bold face type) equal to the Laplace transform of the corresponding physical potential and current. Since we are dealing only with sinusoids, the complex numbers which represent the physical current and voltage have particularly simple meaning: the amplitude of the complex number is the amplitude of the sinusoid, and the phase of the complex number is the phase of the sinusoid. Similarly, the real part of the complex number is the in-phase component of the sinusoid and the imaginary part of the complex number is the out-of-phase (that is, quadrature) component of the sinusoid.

where V_{obs} is the output voltage of the amplifier; I_V is the sum of the current flowing from the microelectrode and the current flowing from the capacitance C_V into the node at the inverting input of the amplifier (this node is labeled ε in Fig. 1); C_1 is the feedback capacitance indicated in Fig. 1 (feedback network A); and C_g is the capacitance between the inverting input of the amplifier and ground. Eq. 2 has been derived using the fact that in almost all cases

$$\omega_c C_1 \gg (1/R_1) + (\omega_c C_g/A_o) \tag{3}$$

In the analysis of the whole circuit of Fig. 1 (in contrast to the above analysis of just the input amplifier) one must consider the effects of C_V as well as C_g. It is useful to note that the noise and stability of the output voltage V_{obs} depends on C_V and C_g in much the same way. Thus one may, in a spirit of approximation, extend the following discussion of the input amplifier to that of the whole circuit by replacing C_g with $C_g + C_V$.

Eq. 2 describes the response of a second order system with natural frequency ω_n and damping ζ where

$$\omega_n = \left[\frac{\omega_c}{R_1(C_1 + C_g)}\right]^{1/2}; \qquad \zeta = \left[\frac{C_1}{2}\frac{R_1\omega_c}{C_1 + C_g}\right]^{1/2}. \tag{4}$$

Examination of the transient and sinusoidal response of such a system (Clark, 1962, pp. 69, 332) shows that the damping is closely related to the stability and noisiness of the circuit.[2]

If the damping is small, as when the feedback capacitance C_1 is small, there is a large resonant peak in the amplitude response of the circuit, the circuit is noisy, and the output tends to be unstable. It is therefore impossible to reduce C_1 arbitrarily with realistic operational amplifiers, and indeed most operational amplifiers will oscillate if C_1 is reduced below 0.1 pF.

We can then summarize the problems in designing the feedback network. The feedback capacitance must be very small in order to allow sufficient bandwidth; on the other hand, it must be reasonably large to ensure freedom from noise and oscillation. The operational amplifier should be chosen to have maximum bandwidth ω_c, minimum input capacitance C_g, and must be well represented by Eq. 2. This last specification is important since most operational amplifiers have more phase shift than stated by Eq. 1 and so the output tends to be more unstable and noisy than predicted by Eq. 2. We have found three amplifiers which fulfill these requirements reasonably well (Models 1011, 1027, and 1025 of Teledyne Philbrick, Dedham, Mass.) although the last of these, which is the best in other respects, has somewhat too much current noise for our present purposes.

Even with these amplifiers, and the lowest practical feedback capacitance (about 0.3 pF), the artifact produced by feedback network A is unacceptable, the phase shift being more than 10° at 10^4 Hz, and more than 1° even at 1,000 Hz. Because of this problem we have used another more complicated feedback network (shown in Fig. 1 as feedback network B; Pease, 1969) which has much less phase shift than network A at angular frequencies below $1/R_1C_1$. Indeed, network B introduces a phase shift of arctan $(\omega R_1C_1)^3$ and allows a phase shift of

[2] By noisiness we mean the total root mean square (rms) noise, referred to input, in the frequency range DC – 100 KHz.

[3] A full analysis of feedback network B, including the effects of the finite gain of the operational amplifier and the effects of the capacitance C_g, has been carried out as described above for feedback network A. The analysis is not presented here, since it does not result in any new conclusions concerning the choice of the operational amplifier, and because the resulting expressions are too clumsy to admit physical interpretation, without numerical analysis and root locus techniques.

about 1° at a frequency of 10^4 Hz with a feedback capacitance of 0.28 pF, a 10-fold improvement over network A. Network B does introduce some additional noise into the output V_{obs} both because it has greater bandwidth than network A (with a given feedback capacitance) and because it has a small peak in its amplitude response. The circuit is stable—we have never observed either parasitic or sustained oscillation—and the small additional noise has not been a problem.

It is important that the resistors chosen for either feedback network be reasonably pure circuit elements. We have used ordinary carbon resistors since they behave essentially as a resistor in parallel with a capacitance. Deposited carbon or metal film resistors would be less noisy but are often quite impure circuit elements. The resistance element inside such resistors is often cut into a spiral; the capacitance between the turns of the spiral is appreciable and makes the resistor have a rather complicated frequency response. Feedback network B is much less sensitive to these problems than network A provided the two resistors have similar frequency response.

One might expect that a more complicated feedback network would allow further improvement in the phase response for $\omega < 1/R_1C_1$. R. Mathias has shown, however, that no RLC feedback network will allow further improvement (personal communication).

Feedback network B does pose one new problem, however: one of the capacitors (the variable capacitor in feedback network B of Fig. 1) must be adjusted to a certain value, $4C_1$. Analysis of the circuit shows that the adjustment is not critical; that is, the performance of the circuit is still adequate even if the capacitor is misadjusted by 5%. Nonetheless, the method by which the circuit element is adjusted is most important since several of the obvious procedures have dangerous pitfalls.

The essential problem in designing a calibration procedure is to apply a *known* current to the node at the inverting input of the operational amplifier. It is not possible to apply this current by connecting one end of a resistor to the input and the other end to an oscillator for three reasons. First, if the resistor is large (of the order of $10^5\ \Omega$) the stray capacitance across the resistor will be important at frequencies of interest. Second, if the resistor is smaller than $10^5\ \Omega$, it will significantly change the frequency response of the input amplifier. (This can be shown by extending the analysis summarized in Eq. 2 to include such a resistance. It turns out that the resistance, if sufficiently small, has a significant effect on the coefficient of s in the denominator of Eq. 2.) Third, the very process of connecting the resistor to the input significantly changes the stray capacitances in the experimental apparatus, especially C_g.

We have used a procedure which is not subject to these problems (see Schneider, 1969). If a wire connected to the output of the oscillator is placed some 1 cm from the input of the operational amplifier, current can flow into the input through the capacitance between the wire and the input (about 0.2 pF). This additional capacitance is the only change in the setup associated with the measurement and is not likely to be important since it is small compared with either C_V (about 10%) and C_g (about 5%). The current flowing through the air capacitance into the node at the inverting input is 90° out-of-phase with the oscillator voltage (of amplitude $|V_s|$) since the voltage ε on the inverting input of the operational amplifier is negligible. One then adjusts the variable capacitor so that the phase of the output is also −90°. The deviation of the phase from −90° is a measure of the total error in the circuit and is an excellent test of the whole input amplifier circuit. Fig. 2 (curve A) shows the results of such measurements. It can be seen that the maximum phase error from all causes is 1° at frequencies above 100 Hz. The residual phase error in the input amplifier is stable within 0.1° over 1 yr and so can be subtracted from the experimental records.

The phase error at the lower frequencies shown in Fig. 2 is measured with a resistor connected to the input. There is no significant difference between the measurements with the resistor and with the

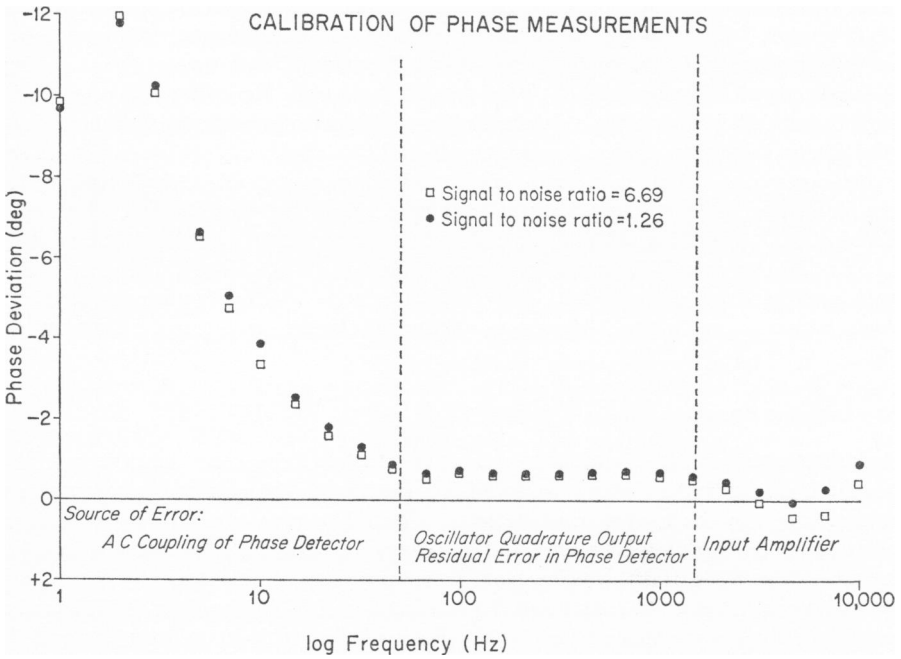

FIGURE 2 Calibration of apparatus. Current of known phase was injected at the node labeled ε in Fig. 1. At frequencies below 215 Hz the current was injected through a resistor. At frequencies above 68 Hz current was injected through an air capacitor. In the overlap region between 68 and 215 Hz, the phase deviations measured were the same within 0.2°. The sources of phase error are indicated. The entire phase curve was reproducible within 0.2° over a period of 2 yr. The only error expected to vary with experimental conditions is the residual deviation in the phase detectors since this in principle should depend on the character of the signal and noise. Two curves taken at different signal to noise ratios show that such variation is not significant here.

air capacitor in the frequency range 68–215 Hz. The phase error at low frequencies is caused by the AC coupling networks in the phase detectors and is also stable over a 1 yr period. It can be subtracted from the experimental records. The phase error in the frequency range 46–1,000 Hz is caused by two factors. About half of the error is caused by phase deviations in the quadrature output ($\cos \omega t$) of the oscillator and about half is caused by the imperfect behavior of the phase detectors in the presence of noise. The first half of the error is stable over 1 yr and so can be subtracted from the experimental records. The second half of the error represents a real uncertainty in our experimental results since it is not expected to be constant and in fact should depend on the amount of noise, the amplitude, and the phase of the signal.

Finally, we should mention that it is not wise to test the input amplifier by connecting a capacitor between the input of the operational amplifier and the output of the oscillator for two reasons: first, the wires of the capacitor change the stray capacitances and second, greasy fingerprints on the case of the capacitor produce a resistive shunt significant at frequencies below 1,000 Hz.

There are several practical difficulties with the input amplifier circuit shown in Fig. 1. The DC gain of the amplifier (the output divided by the potential at the tip of the voltage recording microelectrode) depends on the resistance of the microelectrode and so changes with time. For this reason we measure the gain (and at the same time the resistance of micro-

electrode) many times during the course of an experiment. A convenient method of measuring gain is to apply a DC potential to the noninverting input of the current amplifier (see Fig. 1). The amplifier then drives the bath to the same DC potential, and the output of the input operational amplifier is proportional to the gain of the circuit. Another disadvantage of the circuit is that the fiber impedance is shunted by the resistance of the microelectrode. This does not produce an important change in resting potential or viability but it does introduce some error into our results at low frequencies where the loading magnitude of the fiber impedance is large (Schneider, 1970). We consider this loading effect in some detail below.

There is a further problem with this input amplifier which we have not been able to analyze in such a satisfactory way. The amplifier output is sensitive to the electrical properties of the voltage recording microelectrode and, if the microelectrode behaves in a nonlinear manner, it will introduce phase shift and the output voltage will be distorted (see the Appendix and Fig. 5).

Method of Measurement of Sinusoids

The accurate measurement of sinusoids over a wide range of frequency requires careful attention to detail, particularly if the sinusoid is contaminated with noise. In our situation the sinusoid recorded by the voltage microelectrode is heavily contaminated by noise, the signal to noise ratio being typically between 1 and 3. (The noise we measure is around 800 μV rms in the bandwidth DC – 100 kHz. The signal is typically 1 mV rms.)

Previous measurements (Falk and Fatt, 1964; Eisenberg, 1967; Schneider, 1970) have been made from oscilloscope displays, the vertical plates of the oscilloscope being connected to one sinusoid and the horizontal plates to the other. The resulting Lissajous figures, as they are called, can be read with surprising reproducibility even in the presence of some noise, but systematic error is introduced so the absolute accuracy of the measurements is poor (Benson and Carter, 1950). Measurements have also been made with phase meters (Freygang et al., 1967) which rely essentially on the average of many zero crossings and are subject to bias in the presence of noise. Neither of these measuring systems were tested to determine the accuracy of the measurements in the presence of noise.

We have measured the amplitude and phase using quite a different principle based on the idea of synchronous detection (or, as it is often called, phase-sensitive detection) widely used to recover signals from large amounts of noise (Danby [1970] includes a detailed discussion of the operation of these detectors). Phase-sensitive detectors use a reference signal (which must be a sinusoid hardly contaminated by distortion or noise) to switch the incoming noise signal. The resulting switched sinusoid plus noise is then applied to an integrator. The response of such a phase detector is ideally $|V| \cos \phi$ where $|V|$ is the amplitude of the signal. input and ϕ is the phase difference between the signal and reference: an ideal phase detector measures the inphase component (also called the real part) of the signal, essentially independent of noise. In order to determine both the phase angle and amplitude one needs another measurement, most conveniently of the out-of-phase (also called the quadrature or imaginary) component of the signal. A simple way to measure this component is to shift the phase of the reference by 90°. The phase detector then measures $|V| \sin \phi$, the imaginary part of the signal. Thus, the phase detectors measure directly the real and imaginary parts of the signal. The phase angle and amplitude can then easily be calculated. We derive the in-phase and the quadrature reference signal directly from one oscillator (model 4001, Krohn-Hite Corp., Cambridge, Mass.); the phase accuracy of the quadrature output of this oscillator is 0.25° and the distortion of the sinusoid is essentially unmeasureable, less than 0.01%. These two reference signals are applied to two phase detectors (Brookdeal Model 411, Brookdeal Electronics Ltd., Bracknell, Berks.) each of which receives the same input signal and so the two

components of the signal are measured simultaneously. The outputs of the two phase detectors are read by a digital voltmeter and printed.

The important consideration in this arrangement is the accuracy of the phase detectors themselves both in the presence and absence of noise. The phase detectors can be calibrated in the absence of noise by applying a signal 90° out of phase from the reference and observing the output, which should then be zero. A convenient and very accurate (better than 0.01°) method of shifting phase 90° is to use a differentiator at low frequencies (below 1,000 Hz) or an integrator at high frequencies, each circuit being made with operational amplifiers (Graeme et al., 1971). We have used that method as well as the method discussed above (Fig. 2). Curve A, Fig. 2, shows the total phase error in the input amplifier, oscillator, and phase detector with a signal to noise ratio of 6.7:1 (rms signal to rms noise in 100 kHz bandwidth). Curve B shows the total phase error with a signal to noise ratio of 1.3:1.

It is most important to check phase-sensitive detectors by this or an equivalent method since several detectors currently available have severe phase shift in the absence of noise, which changes significantly in the presence of noise. Indeed, in order to achieve the accuracy illustrated the Brookdeal phase detector had to be modified. On the suggestion of Dr. W. New, we take the output of the phase detector directly from the emitter of the output transistor of the integrator, avoiding internal pickup caused by the protective resistor normally present in the output circuit.

Capacitive Artifact

The experimental arrangement described above (Fig. 1) is subject to several forms of capacitive artifact. The most obvious source of artifact is the current flow through the capacitance C_c which couples the current passing microelectrode to the voltage recording microelectrode. Because the oscillator output voltage V_s is much larger than the potential inside the muscle fiber, the current through the coupling capacitor, which is $j\omega C_c V_s$, is appreciable even for very small values of capacitance. We have eliminated this source of difficulty by reducing C_c to 1.78×10^{-17} F, a typical value determined by direct measurement with the current microelectrode placed just as in an experiment and the voltage microelectrode placed in air just above the bathing solution. The capacitance was reduced to this value by coating the current passing microelectrode down to some 150 μm of the tip with a highly conductive paint containing colloidal silver (a number of such paints are satisfactory; Electrodag 415 or 416, manufactured by Acheson Colloids Co., Port Huron, Mich. are quite convenient to use) and then connecting the coating to ground. The coating is toxic and so it is necessary to cover the silver paint with a layer of varnish (for instance, No. 37-4 made by GC Electronics, Rockford, Ill.). This varnish also electrically insulates the silver coating from the bathing solution.

Once the coupling capacitance has been reduced to a negligible value, it might seem that there should be no further capacitive artifact (Freygang et al., 1967; Schneider, 1970) and this would be the case if the extracellular solution bathing the preparation were at a uniform potential independent of position or frequency. Direct measurement of the potential of the bath (most realistically performed with the current microelectrode inside the fiber) shows a significant extracellular potential which depends strongly both on frequency and position, being largest at high frequencies and near the current microelectrode. There are three possible causes of the extracellular potential in our experimental arrangement. First, it could be caused by current flow through the capacitance of the wall of the microelectrodes (C_V and C_I in Fig. 1) and through the resistance of the bathing solution. Second, it could be caused by current flow through the membrane of the muscle fiber and then the bathing solution. Third, the frequency dependence but not the spatial dependence could be caused by current flow through the impedance of the bath electrodes.

The last effect can be measured by placing a voltage recording probe, which need not be a microelectrode, far from the muscle fiber and far from the current passing microelectrode. We have reduced the bath potential measured this way to a negligible value (less than 0.05% of the potential inside a fiber) by reducing the impedance of the bath electrodes as suggested by Adrian et al. (1970). Our bath electrodes consist of a parallel combination of a Pt/Pt black electrode, which has very low impedance (and that impedance decreases as $\sqrt{\omega}$ as ω increases) and a Ag/AgCl electrode, which unlike the Pt/Pt black electrode has a stable DC potential and a definite impedance at low frequencies.

The circuit developed by Eisenberg, and used by Schneider (1970), in principle keeps the potential in the bath small by negative feedback from the output of an operational amplifier. If the circuit is analyzed in detail, using Eq. 1 to represent the operational amplifier, the bath potential can be shown to be significant: the potential in the bath is always the output voltage of the operational amplifier divided by $A(j\omega)$, as defined by, say, Eq. 1. Since $A(j\omega)$ decreases in magnitude at least linearly with frequency while the output voltage stays more or less constant, there must be some frequency at which the bath potential becomes important. This frequency is quite low for the operational amplifier used by Schneider and is below 10,000 Hz even for the wide-band operational amplifiers available today. The circuit also causes noise and stability problems and so, for all these reasons has been avoided.

We have not been able to measure directly the component of the extracellular potential produced by current flow across the membrane nor have we been able to predict the extracellular potential theoretically because of mathematical difficulties associated with the cylindrical geometry of a muscle fiber. Such theoretical predictions are available for spherical cells (Peskoff et al., 1972)[4] and in that case the extracellular potential produced by the membrane current would be expected to be quite small but not negligible. The analysis shows that the transmembrane potential, or indeed the potential anywhere inside the cell with respect to the potential immediately outside the cell, is unaffected by the extracellular potential. The correct procedure for determining the electrical properties of the cell interior and membranes in the presence of an extracellular potential produced only by the membrane current is to measure the potential inside the cell and subtract from it the potential immediately outside the cell, the current source being in the same position inside the cell for both measurements.

We next consider the extracellular potential caused by current flow through the capacitance of the wall of the microelectrode and the resistance of the bath solution. It is useful to determine the expected size of this effect before proceeding to the somewhat involved exact analysis. The capacitance C_I and the bath resistance R_b form a voltage divider (or a differentiator if you will) which attenuates the oscillator voltage by a factor of approximately $j\omega C_I R_b$. C_I would be about 2 pF if the microelectrode were not shielded; and R_b can be estimated by the "convergence" resistance expected from current flow in a large conductive medium, the shank of the microelectrode being approximated as a cylindrical source of current (Eisenberg and Johnson, 1970, Eq. II.1–10). R_b is expected to be about 200 Ω for a microelectrode with a shank diameter of 10 μm in a solution with a resistivity of 80 Ω-cm. The extracellular potential would then be expected to be 2.5×10^{-5} times the oscillator voltage at a frequency of 10,000 Hz. Since the oscillator voltage is larger than the internal potential by a factor of about $(R_I/|Z|) \simeq 23{,}000$ at 10,000 Hz, it can be seen that the external potential would be expected to be about 60% of the internal potential. This is about half of the value of the extracellular potential observed with unshielded microelectrodes, the rest of the potential being caused by the other effects discussed previously and by current flow through C_V.

[4] *Note added in proof:* A. Peskoff has just completed a similar analysis for a cylindrical cell.

When the current microelectrode is coated with a conductive paint to within some 150 μm of the tip, the capacitance C_I is reduced by a factor of about 15. If the voltage microelectrode were also shielded in this way, the capacitive artifact caused by the bath potential would be negligible in Ringer solutions of normal conductivity and would still be small in Ringer solutions of reduced conductivity. However, the large increase in C_g produced by such shielding increases the noise and decreases the stability of the input amplifier enough so that we are unable in practice to use shielded voltage recording microelectrodes.[5] The capacitive artifact in our experiments, performed with unshielded voltage microelectrodes, is then significant, especially in solutions of low conductivity.

In order to remove the artifact from our experimental data it is necessary to analyze the lumped equivalent circuit of the apparatus shown in Fig. 1. Application of Kirchoff's laws gives

$$\mathbf{Z} = \frac{\mathbf{Z}_{obs} - R_b(1 - \omega^2 C_V C_I R_V R_I) - j\omega[R_V R_I C_c + R_b(C_V R_V + C_I R_I)]}{\mathbf{L}_f} \tag{5}$$

$$\mathbf{L}_f = 1 - \mathbf{Z}_{obs}\left[\frac{1}{R_I} + \frac{1}{R_V}\right], \tag{6}$$

where R_V and R_I are the resistance of the current and voltage microelectrodes, respectively; C_V and C_I are the capacitances between the inside of the voltage and current microelectrodes and the bath; R_b is the *equivalent* resistance of the bathing solution; C_c is the capacitance which couples the oscillator output to the voltage recording microelectrode; $\mathbf{Z}$ is the impedance of the fiber; $\mathbf{Z}_{obs}$ is defined by measurements with both electrodes in the cell: $\mathbf{Z}_{obs} = (-\mathbf{V}_{obs} R_I R_V)/(\mathbf{V}_s R_1)$; $\mathbf{V}_s$ is the output voltage of the oscillator; $\mathbf{V}_{obs}$ is the output voltage of the input amplifier.

It is convenient to define $\mathbf{Z}_{obs}$ this way since $\mathbf{Z} \to \mathbf{Z}_{obs}$ in the ideal situation where R_I and $R_V \gg |\mathbf{Z}|$, $C_c = 0$, and $R_b = 0$. The real situation is not too far from this ideal case, at least at frequencies below some 800 Hz. In the derivation of Eq. 5 we have made the following assumptions, which introduce errors of less than 0.1% under all conditions of interest:

$$\frac{1}{R_V} + \frac{1}{R_I} \ll \frac{1}{R_b}$$

$$|\omega^2 C_I C_V R_b - j\omega C_c| \ll 1/(R_V + R_I)$$

$$\omega(C_V + C_I)R_b \ll 1. \tag{7}$$

Eq. 5 seems at first to be quite formidable, requiring extensive measurements and computations if it were to be used to remove the capacitive artifact from our experimental results. This is not the case. The denominator of the equation, called $\mathbf{L}_f$, describes the attenuation of the voltage inside the fiber caused by current flow to ground through the two microelectrodes. The next section of this paper describes a simple method of evaluating $\mathbf{L}_f$, which turns out to be quite close to one.

[5] *Note added in proof:* The Philbrick operational amplifier model 1027 has recently been modified to have considerably reduced noise and better stability. Using the modified amplifier, we are now able to shield the voltage microelectrode with conductive paint without important increase in noise or decrease in stability.

The capacitive artifact is described by the rather complicated numerator of Eq. 5, but the numerator can directly be measured by removing the voltage recording microelectrode from the interior of the fiber to a position just outside the fiber, the current microelectrode being left inside the fiber. In that case we measure the real and imaginary parts of $\mathbf{V}_{obs}^{(out)}$, the resistance of the current and voltage microelectrodes R_I and R_V as described in the caption to Fig. 1, and the voltage applied to the current microelectrode $\mathbf{V}_s^{(out)}$. If the microelectrode resistances are independent of frequency (see the Appendix), we can define an extracellular impedance by

$$\zeta_{obs} = -(R_I R_V / R_1)(\mathbf{V}_{obs}^{(out)} / \mathbf{V}_s^{(out)}),$$

and circuit analysis shows that

$$\zeta_{obs} = R_b(1 - \omega^2 C_V C_I R_V R_I) + j\omega(R_V R_I C_c + R_b[C_V R_V + C_I R_I]), \qquad (8)$$

where we have assumed $R_I \gg |Z|$, as it is at the frequencies where ζ_{obs} is significant.

The impedance of the fiber is then simply the difference between the impedance observed inside the fiber and that observed outside the fiber, both corrected by the loading factor, $\mathbf{L}_f$

$$\mathbf{Z} = (\mathbf{Z}_{obs} - \zeta_{obs})/\mathbf{L}_f . \qquad (9)$$

There are three configurations which might be thought to be equivalent methods of measuring ζ_{obs}. In the first configuration, the voltage microelectrode would be just outside the fiber and the current microelectrode would be inside the fiber; in the second configuration, the voltage microelectrode would be inside the fiber and the current microelectrode would be just outside the fiber; in the third configuration, both microelectrodes would be outside the fiber. These are not equivalent, however, and only the first is appropriate. They differ because the extracellular potential near the current microelectrode depends greatly on whether the current microelectrode is inside or outside the fiber (Peskoff et al., 1972). The first configuration is appropriate because it directly measures the extracellular potential produced by all causes (and the distortion of that potential produced by C_I and C_V) under the same conditions that the impedance $\mathbf{Z}_{obs}$ is measured.

The capacitive artifact is sufficiently large, and the analysis sufficiently complex, that it is necessary to have direct experimental check of our method of correction. Such a check is provided in part by testing Eq. 8, which predicts that the imaginary part (the quadrature component) of the potential observed outside the fiber should be strictly proportional to frequency. Fig. 3 shows measurements of this component from a large number of muscle fibers. (We do not check the real part of the extracellular potential since it is small and sensitive to residual errors in the phase sensitive detectors). The data from all fibers has been scaled to pass through 0 at 1,000 Hz and -1 at 10,000 Hz. Plots of data from individual fibers, as well as the averaged data shown, fall on a straight line. The data taken from muscle fibers in a low conductivity Ringer (solution H described in Table I of Valdiosera et al., 1974 *b*) is particularly significant since in these experiments the extracellular potential is some eight times larger than in the experiments in normal Ringer. Fig. 3 suggests that the extracellular potential is proportional to frequency as predicted by Eq. 8.

The circuit shown in Fig. 1 implies that the current through the membrane, the current through C_V, and the current through C_I all flow through *the same* equivalent resistance R_b. While this is an

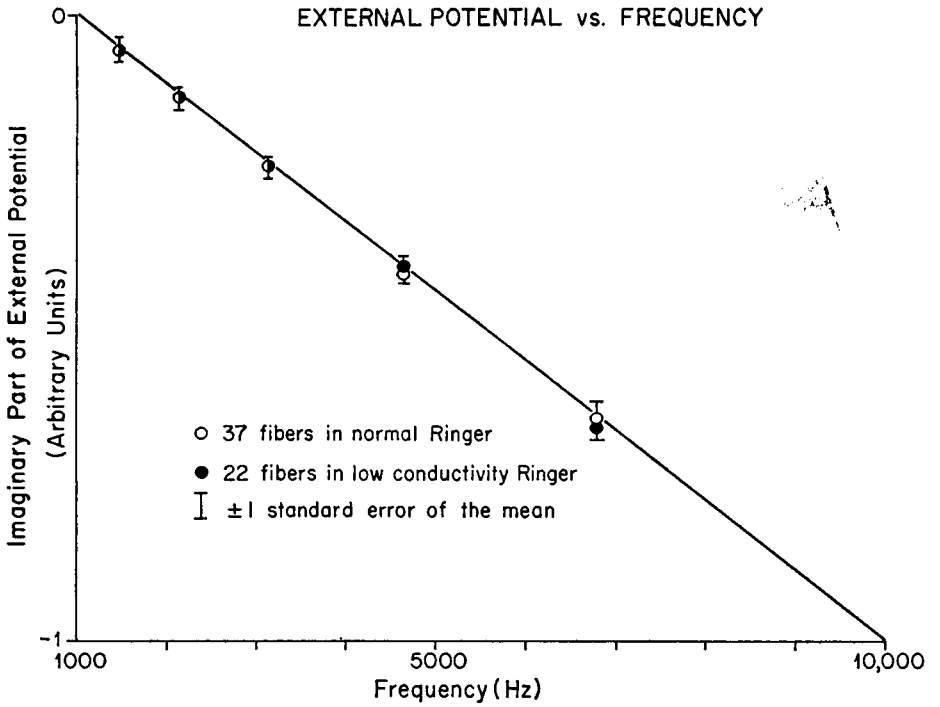

FIGURE 3 Measurement of the imaginary part of the extracellular potential. This experiment serves to test Eq. 8. The nature of the data is indicated; the low conductivity Ringer is solution H described in Table I of Valdiosera et al., 1974 *b*. The data has been scaled arbitrarily to pass through 0 at 1,000 Hz and −1 at 10,000 Hz. There does not appear to be significant deviation from a straight line and we conclude that Eq. 8 is an adequate description of the extracellular potential.

imprecise but reasonable approximation for the capacitive currents, it is an unlikely approximation for the membrane current since the geometry of the source of the membrane currents (as seen by the extracellular solution) is very different from the geometry of the microelectrodes. Nonetheless, the above discussion—based on Peskoff's analysis of the spherical cell—shows that the subtraction procedure of Eq. 9 will correctly remove extracellular potentials arising from current flow across the membrane. Furthermore, the linearity of the results shown in Fig. 3 suggests that most of the extracellular potential is produced by capacitive currents through C_V and C_I.

A difficulty with these corrections is that the extracellular potential is found to vary somewhat with location. It is not really clear which location is the correct one for measuring the extracellular potential; we choose the location immediately outside the muscle fiber with the same angular and longitudinal coordinates as the point at which the internal potential was measured. The correct choice must await an analysis of the cylindrical cell comparable to that of Peskoff et al. for the spherical cell. Some support for our choice can be found in the discussion of Fig. 2 of Valdiosera et al., 1974 *a*.

We conclude then that our corrections for extracellular potential and capacitive artifact

can be justified by direct experimental measurement, but that residual errors in the corrections may be present which could introduce uncertainty into our conclusions.

Procedure for the Capacitive and Loading Corrections

The most obvious and precise way to apply these corrections would be to measure all the parameters in Eqs. 8 and 9 and then apply Eq. 9 directly. The parameters in Eq. 8 might be determined by direct measurement (in the case of R_V and R_I) and then by fitting the equation to a plot of ζ_{obs} as a function of frequency. We have tried this approach but have found it unworkable because the real part of the extracellular potential is negligible except at the highest frequencies and so there is not enough data to determine all the parameters. Therefore, we have taken another less precise approach. Outside the cell we measure the real and imaginary parts of the extracellular potential, the voltage applied to the current microelectrode, and the resistance of the current and voltage microelectrodes. Assuming the resistance of the microelectrodes to be independent of frequency (see Appendix), we calculate ζ_{obs}. Inside the cell the real and imaginary parts of E_{obs} are measured and so is R_I; then Z_{obs} can be calculated. Simple subtraction gives the numerator of Eq. 9. This procedure is precise if the circuit parameters do not change when the current microelectrode is withdrawn from the cell. There will be some error introduced if the circuit parameters change, but we reject experiments in which the change is large enough to cause difficulty.

The loading factor in the denominator of Eq. 9 could in principle be determined similarly, but preliminary calculation showed it to have hardly any effect on the experimental results (less than 1.1° in every case, typically 0.2°) and so the following approximate method was chosen because of its convenience. Instead of using a measured value of the fiber impedance namely Z_{obs}, we used a value calculated by the method of van Valkenburg described above. A circuit model was fit to the observed phase data (Valdiosera et al., 1974 *a*, *b*) and the parameters of the circuit, together with measurements of the DC length constant, input resistance, and microelectrode resistance, allowed calculation of the fiber impedance and thus of the loading factor. This method could be applied even if some of the required data were missing or inaccurate in a particular experiment. In that case average data could be used without introducing significant error since the correction itself is so small.

RESULTS

Fig. 4 shows experimental results from 12 muscle fibers in normal Ringer solution at a sarcomere length of 2.0 μm. The upper part of the figure shows results from two fibers, chosen to show the *extremes* in the shape of the phase plot: these fibers have the least and greatest dip in their phase plots. The open symbols are the raw experimental data; the filled symbols are the data after correction for extracellular potential. Measurements were made at a frequency of 10 Hz four times during the course of the experiment in order to determine the drift in the properties of the preparation. The results shown in the lower part of the figure are the mean on the results from 12 fibers. Each phase point represents the mean (shown ± 2 SE) of the phase measured at that frequency from all 12 fibers. The interpretation of such averaged data is discussed in Valdiosera et al., 1974 *b*. The size and importance of the correction for extracellular potential is apparent, and the reproducibility and reliability of the data, especially in the upper frequency range, can be evaluated.

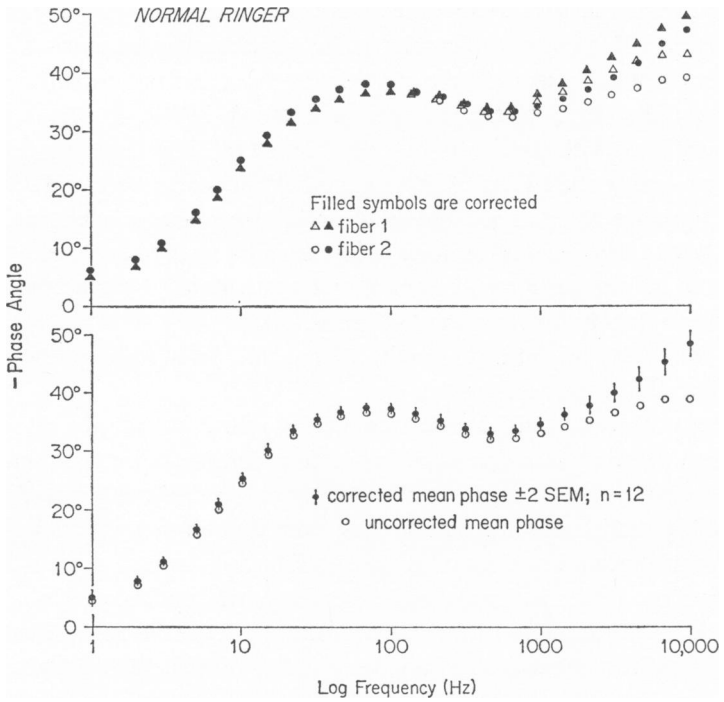

FIGURE 4 The phase characteristic of muscle fibers in normal Ringer. The upper part of the figure shows the phase characteristic from two fibers, chosen because they represent the *extremes* in behavior observed; the size of the dip in the curve is the greatest and the least observed. The open symbols represent the raw measured phase, corrected only for the phase shift in the apparatus (see Fig. 2). The filled symbols represent the phase corrected for the extracellular potential and the loading effect. The lower part of the figure shows the average phase characteristic of 12 fibers. Each phase point (shown ±2 SE) represents the mean of the phase observed from all 12 fibers at that frequency. The sarcomere length of the fibers was 2.0 μm.

DISCUSSION

Improvements in Apparatus

The experimental apparatus described in this paper permits some significant improvements in the measurement of the impedance of physiological preparations.

(*1*) The capacitive artifacts which have plagued earlier measurements have been considerably reduced. In particular, the interelectrode capacitance is some 100 times smaller than in earlier measurements, because we shield the current microelectrode with conductive paint.

(*2*) The importance of extracellular potentials produced by current flow across the wall of the microelectrode and through the resistance of the bathing solution becomes apparent only when the artifact produced by interelectrode capacitance is negligible, and so previous investigations have not considered this problem. The

experimental results in Fig. 4 show that there is considerable extracellular potential even with our shielded current microelectrode; earlier measurements with unshielded current microelectrodes would be expected to have unwittingly included an extracellular potential some 5–10 times larger than shown in Fig. 4. The data shown in Fig. 3 are consistent with the theory described in the text and thus support our simple method of removing the effects of the residual extracellular potential.

(*3*) The input amplifier circuit allows accurate phase measurements at frequencies up to 10 kHz and has reasonable noise, while keeping negligible the effective capacitance to ground. Furthermore, the small error introduced by the amplifier can be measured reproducibly over a period of years.

(*4*) Measurements of the nonlinearity of the microelectrodes allow an estimate of the uncertainty introduced by this error.

(*5*) The use of phase sensitive detectors to measure impedance allows accurate measurements to be made in the presence of considerable noise. The time necessary to analyze the experimental results is also greatly reduced. Furthermore, it is possible to use quite high resistance microelectrodes, even though they are necessarily noisy.

(*6*) High resistance microelectrodes are less likely to damage muscle fibers and so measurements can be made from muscle fibers in good condition.

(*7*) Finally the entire apparatus and procedure allows the convenient and rapid determination of the impedance of a large number of muscle fibers in a number of conditions (see Valdiosera et al., 1974 *b*).

General Physiological Significance

One of the important topics in electrophysiology is the analysis of the electrical activity of cells and tissues with complex structure. It is reasonable to expect the complex structure of such cells and tissues to be intimately related to their function, each part of the cell or tissue having a particular role. A fairly direct way to determine the properties of each part of the cell is to determine the equivalent circuit of the cell and attribute each component of the equivalent circuit to a particular anatomical structure. There is a certain amount of ambiguity in this method, as in any other, but it seems more direct than most other methods available (Valdiosera et al., 1974 *a*, *b*).

The equivalent circuit is determined from impedance measurements which require information of considerable precision over a wide range of frequencies. The methods used to measure impedance must therefore be fairly elaborate and carefully designed for maximum accuracy and it is necessary, in our opinion, to present objective evidence of the accuracy of experimental apparatus as shown in Figs. 2, 3, and 5.

The justification for the detailed consideration of methods given in this paper is the requirement for accuracy and bandwidth in determinations of the equivalent circuit of cells of complex structure. It is also hoped that some of the techniques

developed here will be useful in other experiments which require measurements at high frequencies or short times. In particular, these techniques may be helpful in voltage clamp experiments, which require good high frequency behavior for stability.

The methods presented here have been used to measure the equivalent circuit of some 140 muscle fibers in a number of conditions. The experimental work, and its implications for muscle physiology, are presented in two other papers, Valdiosera et al., 1974 *a, b.*

APPENDIX

Phase Shift in the Microelectrodes

The analysis presented in the text assumes linear behavior of both the microelectrodes and the muscle fiber. Because the equipment used in these experiments does not provide a direct measure of the nonlinearity of the voltage waveform it has not been possible to routinely test this assumption; rather it is necessary to follow the less satisfactory procedure of discussing and justifying it. The current passing microelectrode certainly behaves in a nonlinear manner if the current passed is sufficiently large, and the nonlinearity would contaminate our results by introducing a spurious phase shift. It is relatively easy to reject nonlinear current microelectrodes: we routinely monitor the waveform of the current passed by displaying the output of the current amplifier shown in Fig. 1 on an oscilloscope and checking the symmetry of the waveform. In order to determine the sensitivity of this display to nonlinearity we have measured the second harmonic content of "typical" acceptable microelectrodes and found it to be very small (less than 0.5%). While it is sometimes necessary to reject microelectrodes because they are grossly nonlinear, small adjustments in the location of the microelectrode inside the fiber often will remove this nonlinearity. Furthermore, we fill our current passing microelectrodes with a mixture of K^+ citrate ($\sim$1.8 M) and KCL ($\backsim$0.8 M) since such microelectrodes often have quite low resistance and are sufficiently linear. Finally, measurements made at two different signal levels only differ by 1–2°, even if the current microelectrode is obviously nonlinear.

The phase shift introduced by the voltage recording microelectrode, produced by linear or nonlinear phenomena, is much more difficult to measure (Fig. 5). At low frequencies a simple procedure is to apply a signal to the bath and measure the phase shift of the current flowing through the microelectrode by measuring the phase shift of the output voltage of the input amplifier. If the microelectrode behaves as a resistor, the phase shift would be zero.

The phase shift in the voltage recording microelectrode at high frequencies is difficult to measure because it is so sensitive to stray capacitances. After many attempts, we have devised an experimental arrangement which mimics the arrangement used to measure the potential inside the muscle fiber and yet allows direct measurement of the phase shift of the microelectrode at high frequencies. We use a shielded voltage microelectrode (and increase the signal level to compensate for the extra noise) and coat the tip of the microelectrode with a thin (less than 1 μm) layer of silicone oil to prevent the formation of a meniscus. The bath is carefully shielded from the lead which connects the voltage recording microelectrode and the input operational amplifier. The microelectrode is inserted into the solution to a depth comparable to its depth within a muscle fiber (5–20 μm) in an experiment. The results are shown in Fig. 4 and strongly support the theoretical expectation (Engel et al., 1972: p. 374–375) that the only significant phase shift is that produced by nonlinearities.

These results can give some idea of the phase shift introduced by the voltage recording microelectrode, but they cannot be used to quantitatively correct experimental results because

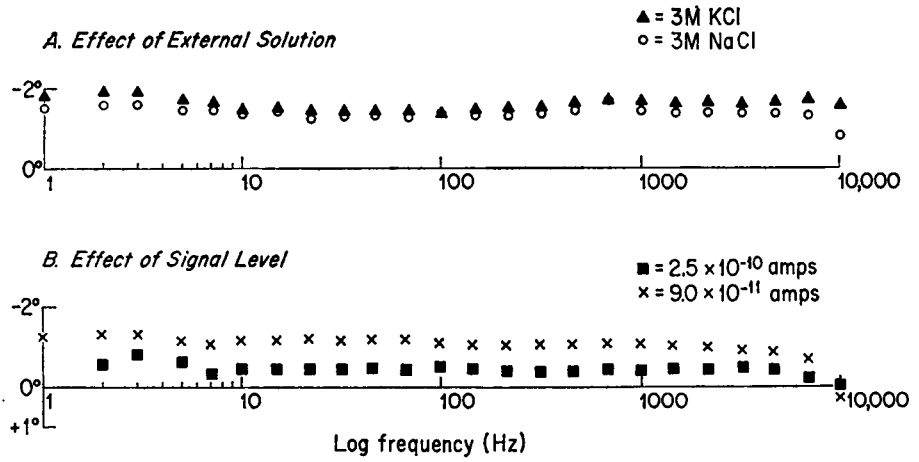

FIGURE 5 The phase shift in the tip of the microelectrode. The results shown serve to place an upper bound on the phase error produced by current flow in the last 5–20 μm of the microelectrode under the conditions indicated. Note that the phase shift is quite independent of frequency. The phase shift depends on the bathing solution and the amount of current and so is probably a reflection of the nonlinear properties of the microelectrode tip. No attempt has been made to investigate these properties in detail.

the phase shift varies with experimental conditions. The phase shift produced by nonlinearity is likely to depend on several variables we cannot control: the tip potential, microelectrode resistance and the bathing solution; it also may depend on the position of the microelectrode inside a fiber and the membrane potential of the fiber. For these reasons the results illustrated in Fig. 4 should be taken only as a likely indication of the size of the phase shift. It would be most desirable to find a method of routinely monitoring the nonlinearity and phase shift in each microelectrode. Digital techniques using stochastic signals may allow such monitoring.

We are indebted to Drs. F. Rasmussen and S. Hagiwara who made it possible for us to work together. Doctors Adrian, Freygang, Mobley, Nakajima, and Peachey kindly sent us unpublished manuscripts. We particularly thank Doctors Leung, Mobley, and Peskoff for their illuminating discussions and searching review of these manuscripts.
This work was supported by National Institutes of Health grant HL 13010.

Received for publication 10 December 1973 and in revised form 4 January 1974.

REFERENCES

ADRIAN, R. H., W. K. CHANDLER, and A. L. HODGKIN. 1970. *J. Physiol.* **208**:607.
BARNA, A. 1971. Operational Amplifiers. Interscience Publishers, Inc. (John Wiley & Sons), New York.
BENDAT, J. S., and A. G. PIERSOL. 1971 Random Data: Analysis and Measurement Procedures. Interscience Publishers, Inc. (John Wiley & Sons), New York.
BENSON, F. A., and A. O. CARTER. 1950. *Elec. Eng.* **22**:238.
BOZLER, E., and K. S. COLE. 1935. *J. Cell Comp. Physiol.* **6**:229.
CLARK, R. N. 1962. Introduction to Automatic Control Systems. John Wiley & Sons, Inc., New York.
DANBY, P. C. G. 1970. *Elec. Eng.* **42**:36.
DESOER, C. A., and E. S. KUH. 1969. Basic Circuit Theory. McGraw-Hill, Inc., New York.
EISENBERG, R. S. 1967. *J. Gen. Physiol.* **50**:1785.
EISENBERG, R. S., and E. A. JOHNSON. 1970. *Prog. Biophys.* **20**:1.

ENGEL, E., V. BARCILON, and R. S. EISENBERG. 1972. *Biophys. J.* **12**:384.
FALK, G., and P. FATT. 1964. *Proc. Roy. Soc. Ser. B Biol. Sci.* **160**:69.
FATT, P. 1964. *Proc. Roy. Soc. Ser. B Biol. Sci.* **159**:606.
FATT, P., and B. KATZ. 1951. *J. Physiol. (Lond.).* **115**:320.
FREYGANG, W. H., and R. GUNN. 1973. *J. Physiol.* **61**:482.
FREYGANG, W. H., S. I. RAPOPORT, and L. D. PEACHEY. 1967. *J. Gen. Physiol.* **50**:2437.
GAGE, P. W., and R. S. EISENBERG. 1969. *J. Gen. Physiol.* **53**:265.
GRAEME, J. D., G. E. TOBEY, and L. P. HUELSMAN. 1971. Operational Amplifiers: Design and Applications. McGraw-Hill, Inc., New York.
HODGKIN, A. L., and S. NAKAJIMA. 1972 *a. J. Physiol.* **221**:105.
HODGKIN, A. L., and S. NAKAJIMA. 1972 *b. J. Physiol.* **221**:121.
JACK, J. J. B., D. NOBLE, and R. W. TSIEN. 1973. Electric Current Flow in Excitable Cells. Clarendon Press, Oxford. In press.
KATZ, B. 1948. *Proc. Roy. Soc. Ser. B Biol. Sci.* **135**:506.
LANCZOS, C. 1957. Applied Analysis. Pitman Medical Publishing Co., Ltd., London.
MOBLEY, B. A., W. H. FREYGANG, and R. H. GUNN. 1973. *Biophys. J.* **13**:195 *a.*
PEACHEY, L. D., and R. H. ADRIAN. 1973. *In* Structure and Function of Muscle. G. Bourne, editor. 2nd edition. In press.
PREASE, R. A. 1969. On feedback capacitance. *Lightning Empiricist.* **17**:13. (Available from Teledyne Philbrick, Dedham, Mass.).
PESKOFF, A., R. EISENBERG, and J. C. COLE. 1972. Potential induced by a point source of current in the interior of a cell. UCLA Engineering Report No. 7259.
SCHNEIDER, M. F. 1969. Linear A.C. cable properties of frog muscle fibers. Ph.D. Thesis. Duke University, Durham, North Carolina.
SCHNEIDER, M. F. 1970. *J. Gen. Physiol.* **56**:640.
TUTTLE, D. F., JR. 1958. Network Synthesis. John Wiley & Sons, Inc., New York.
VALDIOSERA, R., C. CLAUSEN, and R. S. EISENBERG. 1974 *a. J. Gen. Physiol.* **63**:432.
VALDIOSERA, R., C. CLAUSEN, and R. S. EISENBERG. 1974 *b. J. Gen. Physiol.* **63**:460.
VAN VALKENBURG, M. E. 1960. Modern Network Synthesis. John Wiley & Sons, Inc., New York.
ZADEH, L. A., and C. A. DESOER. 1963. Linear System Theory: The State Space Approach. McGraw-Hill, Inc., New York.